Sodium chloride on Si(100) grown by molecular beam epitaxy

Jen-Yang Chung,[1,2] Hong-Dao Li,[1,2] Wan-Heng Chang,[1] T. C. Leung,[3] and Deng-Sung Lin[1,*]

[1]*Department of Physics, National Tsing Hua University, 101 Kuang-Fu Road Section 2, Hsinchu 30013, Taiwan*

[2]*Institute of Physics, National Chiao-Tung University, 1001 Ta-Hsueh Road, Hsinchu 30010, Taiwan*

[3]*Department of Physics, National Chung Cheng University, Chia-Yi, Taiwan 62101, Republic of China*

(Received 19 September 2010; revised manuscript received 17 January 2011; published 25 February 2011)

Sodium chloride (NaCl) films were grown on an Si(100)-(2 × 1) surface at near room temperature by molecular beam epitaxy (MBE). The atomic structure and growth mode of the prototypical ionic materials on the covalent bonded semiconductor surface is examined by synchrotron core-level x-ray photoemission spectrum (XPS), scanning tunneling microscopy (STM), and first-principles calculations. The Si 2*p*, Na 2*p*, and Cl 2*p* core-level spectra together indicate that adsorbed NaCl molecules at submonolayer coverage [i.e., below 0.4 monolayer (ML)] partially dissociate and form Si-Cl species, and that a significant portion of the dangling-bond characteristics of the clean surface remains after NaCl deposition of 1.8 MLs. The deposition of 0.65-ML NaCl forms a partially ordered adlayer, which includes NaCl networks, Si-Cl species, adsorbed Na species, and isolated dangling bonds. The STM results revealed that the first adlayer consists of bright protrusions which form small $c(2 \times 4)$ and (2×2) patches. Above 0.65 ML, the two-dimensional NaCl double-layer growth proceeds on top of the first adlayer.

DOI: 10.1103/PhysRevB.83.085305 PACS number(s): 68.55.J−, 77.55.Px, 68.43.−h, 68.37.Ef

I. INTRODUCTION

The epitaxial growth of insulating films on semiconductor surfaces has attracted much attention due to potential applications in microelectronic and optoelectronic devices, and has aroused scientific interest in the basic principles of epitaxial growth and heterostructure physics.[1–3] NaCl is a prototypical insulator with a large percentage of ionic character. The Si(100) wafers are most commonly used in making Si-based devices and much is known about their surface atomic and electronic structures. Therefore NaCl/Si(100) can be used as a model system for studying the interfacial properties and growth behavior between ionic crystals and a covalent substrate.

Previous studies have established that, under suitable conditions, NaCl can be grown lattice matched to Ge(100) with a high degree of quality.[4–7] A scanning tunneling microscopy (STM) measurement suggests that the growth of NaCl begins with a carpetlike double layer of NaCl film.[5] In an electron energy-loss scattering (EELS) measurement, Zielasek, Hildebrandt, and Henzler found electronic states at the NaCl/Ge interface and suggested that the dimerization of the Ge(100) surface is not eliminated at the NaCl/interface—even if the thickness of the NaCl rises to 20 monolaysers (MLs).[6] The growth mode of the NaCl/Si(100) system has been less studied, perhaps due to the lattice mismatch. The second-nearest-neighbor separation R_1 for a NaCl crystal is 3.98 Å. The surface lattice constant a, or the period of unreconstructed Si(100) 1×1, is 3.84 Å. The lattice mismatch at the heterostructure of NaCl/Si(100) is close to 4%.

Given a large lattice mismatch, the growth of alkali halide on the Si and Ge surfaces at submonolayer coverage does not yield an ordered surface structure. For example, LiBr ($R_1 =$ 3.89 Å) and LiF ($R_1 = 2.85$ Å) are adsorbed randomly onto Si(100) at room temperature. KI (nearest-neighbor separation $R_0 = 3.53$ Å) dissociatively adsorbs on the Si(100) surface at a coverage of less than 0.5 ML.[8] Although thick flat films can be obtained, the growth of KI, LiF, and LiBr on Si(100) and Si(111) surfaces proceeds by the Volmer-Weber (VW) mechanism of island growth as a result of the interfacial lattice mismatch.[8–10] However, Tsay *et al.* found that KCl can grow on Si(100) in a layer-by-layer fashion.[11]

In the present work, NaCl nanofilms were grown by means of MBE and the resulting films were examined *in situ* by high-resolution synchrotron radiation photoemission and STM. *Ab initio* calculations were also applied to model the atomic structure of the first adlayer. Compared to LiF/Si(100) and KCl/Si(100) systems, NaCl/Si(100) has a smaller lattice misfit. Experimental results reveal an unusual growth mode: An adlayer consisting of about 0.65 adsorbed NaCl is formed, followed by a double-layer growth. The first adlayer consists mainly of an NaCl network and unreacted single dangling bonds that form several types of local ordering. These findings demonstrate the richness of growth modes for even relatively simple ionic crystal/covalent crystal heteroepitaxial systems.

II. EXPERIMENTAL DETAILS

A single crystal Si(100) of 1 × 10 or 3 × 10 mm^2 was sliced from an antimony doped wafer with a resistivity of 0.01 Ω cm. The clean Si(100) surface was obtained *in situ* by direct heating to 1450 K for a few seconds after degassing at 900 K for 20 h. NaCl powder of 99.99% purity was evaporated from an alumina crucible by a feedback current flux-controlled electron bombardment beam. Mass spectra have shown that NaCl vaporizes in the forms of NaCl monomer and Na_2Cl_2 dimer molecules; the monomers (majority species) and the dimers (minority species) have partial pressures of the same order of magnitude.[12] The deposition rate was measured by a quartz-crystal thickness monitor. The coverage of NaCl in MLs (denoted by θ) was calculated from the exposure time, assuming the sticking coefficient to be 1. The coverage of 1.0 ML refers to the number of Si atoms on an ideal unreconstructed Si(100) surface with an atomic density of

6.8×10^{14} cm^{-2}. Deposition at a substrate temperature in the range of 300–400 K yields a similar growth behavior; the results reported herein were obtained at approximately 330 K.

The photoemission spectra were recorded in a separated μ-metal-shielded chamber with a based pressure of $\sim 3 \times 10^{-10}$ torr at the Taiwan Light Source Laboratory in Hsinchu, Taiwan. Synchrotron radiation from a 1.5-GeV storage ring was dispersed by a wide-range spherical grating monochromator (SGM). The photocurrent from a gold mesh placed in the synchrotron beam path was monitored to determine the relative incident photon beam flux. Photoelectrons were collected from 45° off normal emission and analyzed by an angle-integrated 125-mm hemispherical analyzer with an acceptance angle of ±8°. The overall energy resolution was less than 120 meV. The STM measurement was taken in a separated UHV chamber with a base pressure of 8×10^{-11} torr. The tunneling current I_t was about 0.1 nA. The topographic height measurement did not strongly depend on the sample bias V_s around −2.4 V typically used. For each of the photoemission and STM measurements, a NaCl nanofilm was prepared *in situ* on a clean Si(100) surface under identical growth conditions in the respective UHV chamber.

III. RESULTS AND DISCUSSION

A. Photoemission results

High-resolution x-ray photoemission spectroscopy can be performed to distinguish between atoms at nonequivalent sites and in different chemical bonding configurations, based on shifts in the atoms' binding energies.[13] Figures 1, 2(a), and 2(b), respectively, present a series of surface-sensitive Si 2*p*, Cl 2*p*, and Na 2*p* core-level spectra for the Si(100)-(2 × 1) surface with various amounts of NaCl deposition. The escape depth for these spectra is estimated to be around 4 Å.[14] Following the standard procedures,[13,15] the spectra were decomposed by least-squares fitting. Briefly, identical Voigt line shapes, each consisting of a pair of spin-orbit split doublets, were used to decompose the Si 2*p* and Cl 2*p* core-level spectra into overlapping components (curves). The solid curves represent the fitting results that overlap the data points. Spectra of the chlorine terminated Si(100)-(2 × 1) [Cl/Si(100)] (bottom, Fig. 1) are also presented for reference. The spectrum has two components, B and Si$^+$, which are separated by 0.90 eV. The B component was responsible for the emission from the bulk atoms and the Si$^+$ component was responsible from the nominal 1.0 ML of the surface Si-Cl species.[16] The corresponding Cl 2*p* spectrum for Cl/Si(100) [Fig. 2(a), bottom] can only be analyzed in terms of a single component that has a pair of split doublets separated by 1.60 eV, implying that all Cl has the same Si-Cl monochloride bonding configuration.

Prior to NaCl deposition, the Si 2*p* spectrum (second from bottom, Fig. 1), which was obtained from the clean Si(100)-(2 × 1) surface, has a component (B) and two components *S* and *S*′, respectively shifted by −0.52 and +0.23 eV. The components *B* and *S* have been attributed, respectively, to emission from the bulk atoms and the up atoms of asymmetric dimers. The origin of the *S*′ component is not

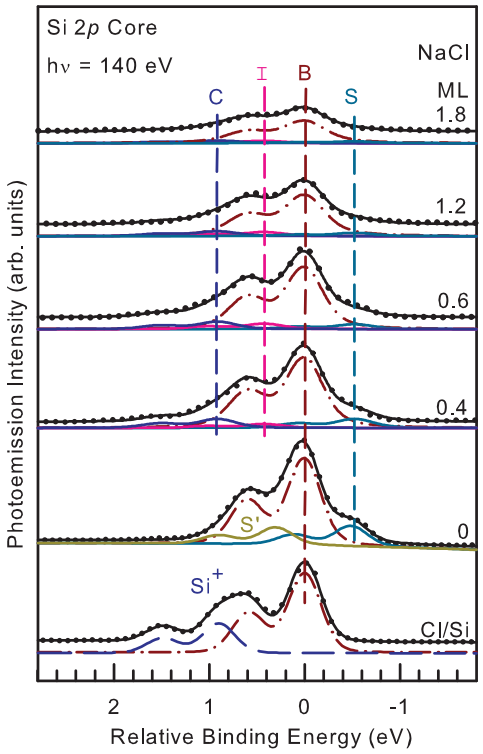

FIG. 1. (Color online) Si 2*p* core-level photoemission spectra (dots) of Si(100) surface with various amounts of NaCl deposition, as specified. The solid curves fit to the spectra. The curves labeled B, S, I, and Si$^+$ are the results, respectively, of the decomposition of the Si 2*p* spectra into contributions from the bulk, the clean surface, the interface layer, and the Si-Cl species. The energy zero refers to the $2p_{3/2}$ bulk position. The dashed lines are guides.

clear, but its energy position is consistent with atoms from the subsurface layers.[17,18] All core-level binding energies are referenced to the bulk Si $2p_{3/2}$ position (99.5 eV) relative to the valence-band maximum.

Figure 1 shows that the intensity of the *S* component in the Si 2*p* spectra declines with increasing NaCl coverage, suggesting a reduction of bare dimers. At $\theta \geqslant 0.4$ ML, a component on the higher binding energy side can be located near the position of the Si$^+$ component. This signature suggests that a portion of the deposited NaCl molecules decompose and Si-Cl bonds are present on the surface. Also, the Si 2*p* spectra become broader, as evidenced by the filling of the two spin-orbital split peaks. Thus two additional components, *C* and *I*, are also included in our fittings and the intensities of the *S, I, C* components are displayed in Fig. 3. Figure 3(a) shows that the intensity of the *B* component I_B decays with increasing NaCl thickness. Fitting of I_B results in a decay length of 1.5 MLs, or equivalently 4.2 Å, which is consistent with the escape depth of photoelectrons with kinetic energy of 40 eV.[14] The coverages (amounts of atoms) that are responsible for both the *I* and *C* components, in MLs, are calculated by comparing their intensity ratios to I_B with I_{Si+}/I_B, assuming that I_{Si+} corresponds to 1.0 ML of the Si-Cl species. The effects of the escape depth and photoelectron diffraction were not corrected. The coverage of *S* is similarly calculated by assuming that the *S* component of the clean Si(100)-(2 × 1) surface corresponds to 0.5 ML of up atoms in bare dimers. The *I* component exhibits

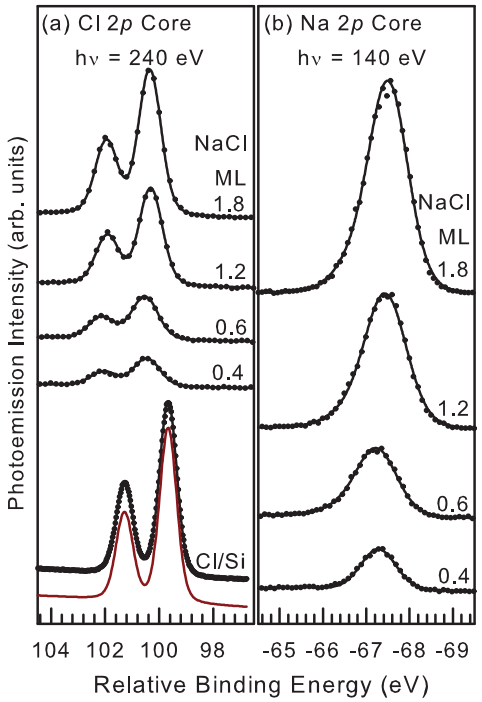

FIG. 2. (Color online) (a) Cl 2*p*, and (b) Na 2*p* core-level photoemission spectra (dots) corresponding to Si 2*p* spectra in Fig. 1. The solid curves fit to the spectra. To eliminate the band-bending effect, the relative binding energies refer to the corresponding Si $2p_{3/2}$ bulk positions in Fig. 1.

a shift of +0.42 eV toward the higher binding-energy side. Its coverage also rises with θ up to 0.38 ML at $\theta = 0.6$ ML, but remains largely constant above 0.6 ML. As will be discussed in Sec. III C, the *I* component is responsible for the Si atoms that are weakly bonded to NaCl clusters.

The fitting results show that the *C* component is shifted from B by +0.90 eV, a value identical to that of the Si^+ peak. Since a large shift commonly results from a large charge transfer,

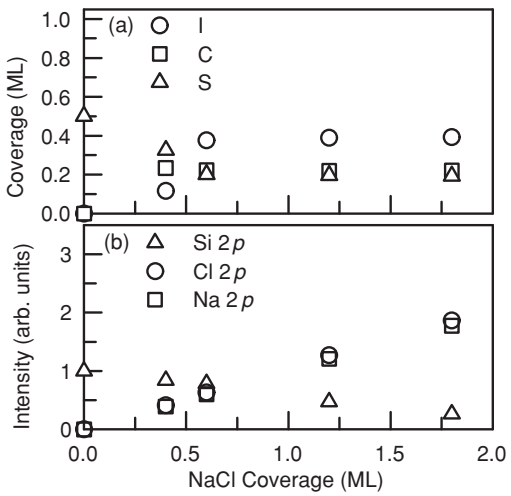

FIG. 3. (a) Coverage evolution of the S, C, and I components in the Si 2*p* spectra. (b) Integrated photoemission intensities of Si 2*p*, Cl 2*p*, and Na 2*p* as functions of NaCl coverage. The estimated error in the deposition rate of NaCl is ±10%.

the *C* component is apparently responsible for the Si-Cl surface species. Accordingly, a fraction of the adsorbed NaCl molecule dissociates. The dissociation energy for the ionic NaCl bond in this molecule is 4.3 eV. The Si-Cl bond energy is −3.94 eV.[19] Calculated adsorption energies for Na adatom on the Si(100)-(2 × 1) surface is about −2.2 eV.[20] Therefore it is energetically favorable for an adsorbed NaCl molecule to dissociate. The intensity of the *C* component or, equivalently, the amount of Si-Cl species or the amount of dissociated NaCl molecules, quickly reaches 0.23 ML at $\theta = 0.4$ ML. As Fig. 2(b) displays, the Na 2*p* spectra exhibit essentially one component for all coverage, suggesting that the charge states of Na, dissociated or bonded with Cl, are nominally +1. However, the Na 2*p* spectra have a comparatively broad Gaussian width of 1.10 eV, compared to that of 0.76 eV found in the Na/Si(100) system.[21] Hidden components with other charge states possibly exist. As Fig. 3 shows, the coverage responsible for the *C* component remains rather constant up to $\theta = 1.8$ MLs but those of Na 2*p* and Cl 2*p* keep increasing with the coverage. These observations suggest that the adsorbed NaCl molecules have a higher probability of dissociating at low coverage, when the dangling-bond pairs (DBPs) are plentiful.

B. STM results

The initial clean Si(100) surface shows an apparent (2 × 1) reconstruction consisting of parallel rows of dimers. Each surface Si atom has one dangling bond. On the vicinal Si(100) surface, two different types of 0.15-nm-high single-height steps, S_A and S_B, separate perpendicular domains of (2 × 1) reconstruction.[22] At the S_A step edges, the direction of the dimer rows on the upper terrace is oriented parallel to the step edge, and perpendicular to the S_B steps. Figure 4 shows a filled-state topographic image for a Si(100) surface after

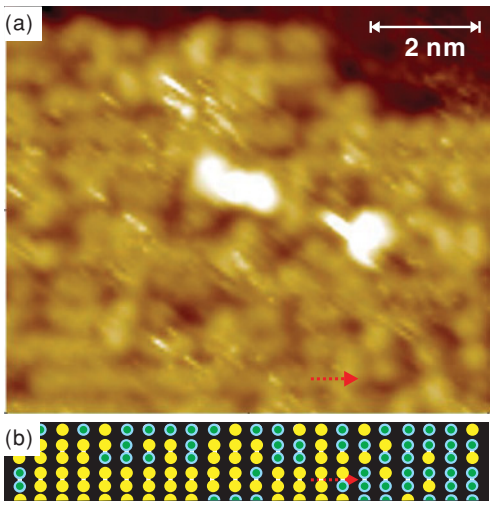

FIG. 4. (Color online) (a) STM images of 0.1-ML NaCl on Si (100) with $V_s = -1.8$ V. The dimer rows running diagonally can be discerned. The two centered bright protrusions are unknown species. (b) Schematic diagram of the bottom area in (a) that expands three dimer rows in width. Yellow (light gray) circles indicate initial dangle bonds; green (dark gray) circles with light blue (light gray) lines indicate adsorption sites. Red dashed arrow lying along a dimer row direction points to a clustered NaCl adsorption site.

0.1-ML NaCl deposition at room temperature. Given a very small amount of coverage, the image is often fuzzy, perhaps due to the presence of surface mobile species (dissociated Na). An NaCl adsorbed site appears dimmer than the bare dimers and often occupies only one side of the dimer. The negative apparent height over the adsorbed sites can be attributed to the reduction in tunneling conductance by bias voltages within the energy gap between the local highest occupied states and lowest unoccupied states around an adsorbed NaCl species.[23] The other end of the reacted dimer appears less affected and has about the same apparent height as the bare dimers (with a pair of dangling bonds). Taking the presence of the *S* component in the Si 2*p* spectra into consideration, the less affected end is likely a single dangling bond (SDB) on a dimer. As Fig. 4 depicts, the SDBs can cluster together, suggesting an ample mobility of the impinging NaCl molecules before adsorption.

Figure 5 shows the evolution of the Si(100) surface after various amounts of NaCl deposition at room temperature. Line profiles, each respectively showing a typical topographic height along the line segment in Figs. 5(a)–5(d), are presented in Figs. 6(a)–6(d). As shown in Fig. 5(a), with increasing NaCl coverage, many (∼0.35 ML) SDBs are visible as bright protrusions after 0.65-ML NaCl deposition. The 0.65-ML NaCl adsorbed species attach preferentially to surface sites and result in a smooth and fully formed layer, referred to below as the first adlayer. No islands are observed at this stage, again suggesting that the adsorbed NaCl species is mobile until a stable adsorption site is found. A zoom-in image [Fig. 7(a)] reveals that most bright protrusions resemble SDBs and that few (0.02 ML) DBPs are present. Small dark areas with missing bright protrusions (SDBs) accounting for about 0.1 ML are assigned as dichloride dimer species, owing to the presence of the Si^{+} component in the Si 2*p* spectra (Fig. 1). Many SDBs form small patches with locally ordered (2 × 2)-*A* [Figs. 7(b) and 7(c)], (2 × 4) [Figs. 7(d) and 7(e)], and (2 × 2)-*B* [Figs. 7(f) and 7(g)] structures. The fractional areas with these ordered structures are summarized as percentages in Table I. More detailed atomic models, including other surface species for these structures, are presented in Sec. III C.

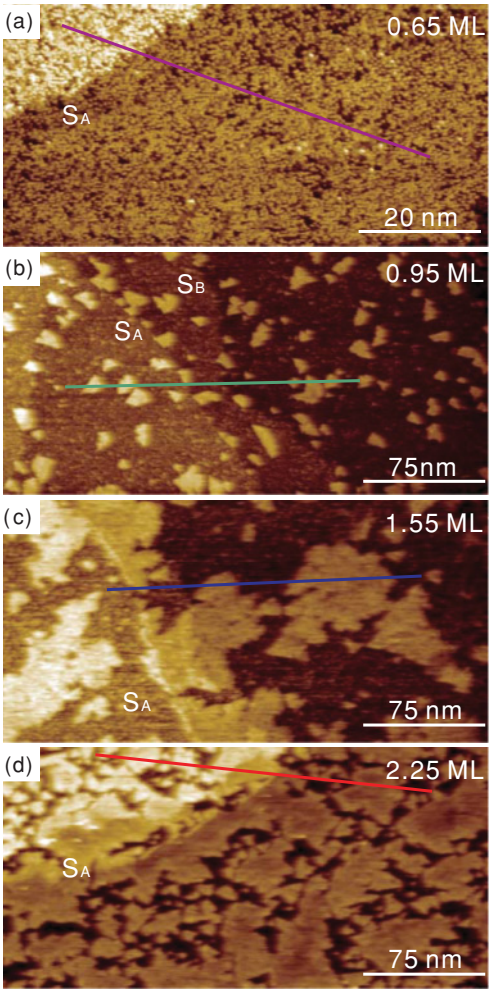

FIG. 5. (Color online) Filled-state STM images showing morphology evolution with various NaCl coverages on Si(100), as labeled. All images are obtained at room temperature with I_t = 0.23 nA and V_s = (a) −2.05, (b) −2.3, (c), and (d) −2.8 V. The images cover an area of about (a) 80 × 40 nm^2, and (b)–(d) 300 × 150 nm^2.

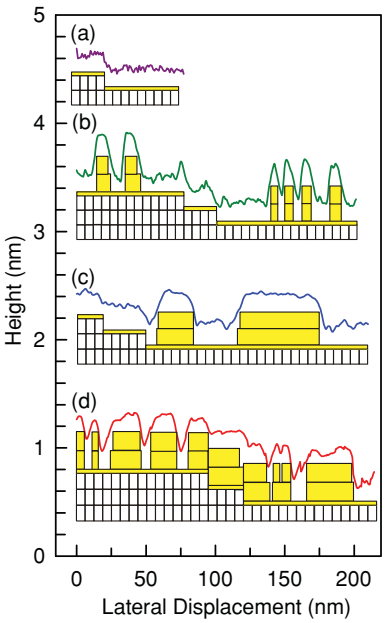

FIG. 6. (Color online) Corresponding apparent topographic height profiles along the line segments in Fig. 5 and schematics of grown NaCl nanofilms. The thin yellow (light gray) layer above the substrate depicts the first adlayer. A thick yellow (light gray) rectangle indicates an NaCl monolayer.

TABLE I. Measured fractional areas, the NaCl coverage, and dangling-bond (DB) coverage in model structures for various patterns and surface species.

Pattern/species	Fractional area (%)	NaCl coverage	DB coverage
Disordered DBs	26		
(2 × 2) *A*	26	0.5	0.5
(2 × 4)	16	0.75	0.25
(2 × 2) *B*	12	0.75	0.25
Cl-Si-Si-Cl	10	0	0
DBP	2	0	0

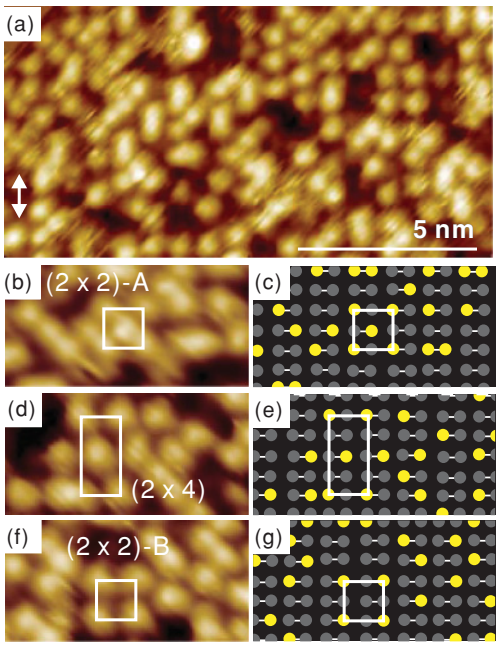

FIG. 7. (Color online) (a) 13 × 7-nm^2 STM images of Si(100) after deposition of 0.6-ML NaCl. The double arrow indicates the dimer row direction. Thermal drift was not corrected. Sample bias voltage used was −2.05 V. (b), (d), (f) Zoom-in images and (c), (e), (g) corresponding schematic diagrams for selective areas on the same sample as that in (a). White rectangles enclose local ordered unit cells as indicated. Yellow (light gray) circles in (c), (e), (g) indicate the positions of bright protrusions. Details of the atomic models are shown in Fig. 9.

Further deposition on the first adlayer leads to the growth of two-dimensional (2D) islands, as shown in Fig. 5(b). In the other words, the first adlayer acts like a wetting layer before further growth. In Sec. III A, photoemission data suggest no further NaCl dissociation above 0.4 ML. Thus the observed 2D patches are NaCl islands; further-adsorbed NaCl molecules migrate on the first adlayer and nucleate into two-dimensional islands. Steps, especially S_A steps, are good island nucleation sites as many islands are attached to steps in Fig. 5(b). As the coverage increases, the 2D islands grow in size and coalesce into large islands, as Figs. 5(c) and 5(d) exhibit. The corresponding line profiles [Figs. 6(b) and 6(c)] show that the 2D islands have an apparent height of about 3.8 Å above the first adlayer. This value, between one and two intralayer Na-Cl distances (2.8 and 5.6 Å) of the NaCl crystal, is about the same as that measured on a double-layer island on Ge(100).[5] The measured apparent height is not sensitive to the sample bias voltage of around -2.5 ± 0.3 V. As depicted in Fig. 8, a well-resolved square lattice with a lattice constant of ∼3.8 Å is observed on top of the 2D islands in Fig. 5(c). This lattice constant is close to the nearest Cl-Cl distance on a NaCl(100) surface. The square lattice vectors are aligned with those of the Si(100) substrate. These observations provide further evidence that the 2D islands are indeed NaCl films of double layer height. Assuming that the 2D islands rest on the first adlayer without removing or adding materials from underneath, the island coverages of 0.18 and 0.50 ML extracted from Figs. 5(b) and 5(c), respectively, account only about

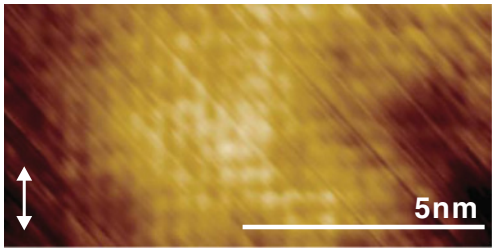

FIG. 8. (Color online) (a) 10 × 5-nm^2 STM image with atomic resolution on top of an isolated island on the same surface as Fig. 5(c). The sample voltage was −2.8 V. The double arrow on the lower left indicates a dimer row direction on the original substrate.

one-half of the additional deposition above 0.65 ML. Together, these considerations including (a) the unchanging coverage of the *C* and *I* components in the Si 2*p* spectra above 0.65 ML, (b) the match between the observed island coverage and the deposition quantity, and (c) the measured topographic height above the adlayer, indicate that those 2D islands are NaCl double layers. Although similarly observed on Ge(100), the double layer in Figs. 5(b) and 5(c) rests on the first adlayer, as opposed to resting directly on the lattice matched Ge(100) surface. It appears that the first discommensurate adlayer serves to release the strain due to lattice misfit between the NaCl and Si interface.

C. Atomic model for the first adlayer

We now discuss the atomic structure of the local ordering in the first adlayer upon the deposition of 0.65 ML of NaCl. At this coverage, STM images and the *S* component in the Si 2*p* spectra indicate that about 0.35 ML of SDBs are present on the surface. Based on the total NaCl coverage and the ordered arrangement of SDBs in Fig. 5, we placed NaCl molecules on top of the clean Si(100) surface, and performed density-functional calculations to determine the relaxed structure and relevant total energy. Prior to relaxation, the initial NaCl molecules were placed 45° with respect to the dimer bond direction with Na ions either near pedestal sites or cave sites. The atomic structures after relaxation are summarized in Figs. 9 and 10. The calculations were based on the Vienna *ab initio* simulation program (VASP) using the

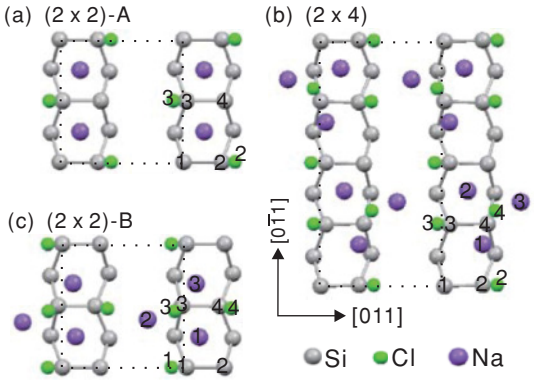

FIG. 9. (Color online) Top views of the relaxed structures for the (a) (2 × 2)-*A*, (b) (2 × 4), and (c) (2 × 2)-*B* ordering. The numbers are atom labels. The dotted line rectangles enclose unit cells.

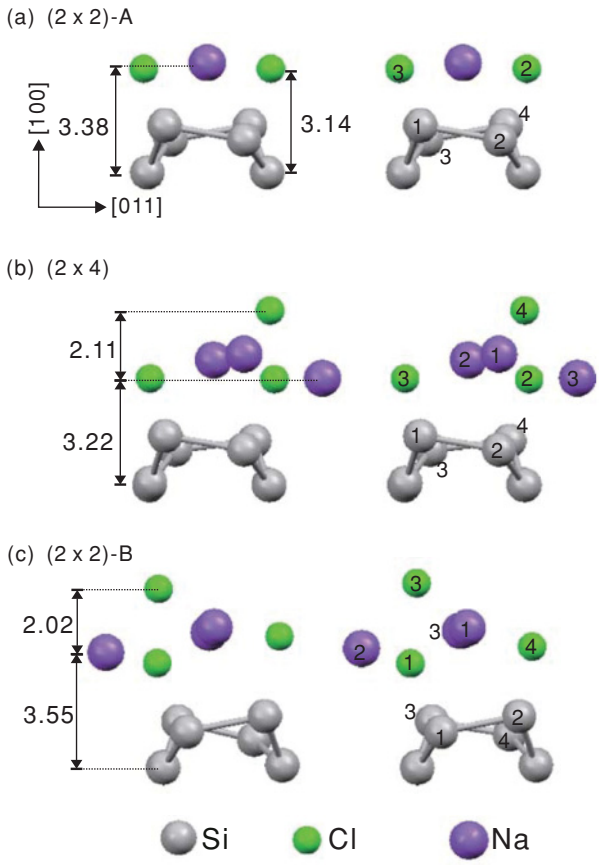

FIG. 10. (Color online) Corresponding side views of the relaxed structures shown in Fig. 9. Distances are given in Å.

projector-augmented wave method and the revised Perdew-Burke-Ernzerhof pseudopotential.[24,25] The Si substrate was modeled by a $4 \times 4 \times 8$ slab, with its bottom surface terminated by hydrogen. A vacuum region of thickness 11.84 Å on top of the Si surface was included to form a supercell. The irreducible Brillouin zone was sampled with a $(4 \times 4 \times 1)$ Monkhorst-Pack mesh, the energy cutoff was set at 400 eV, and the energy convergence was set at 10^{-4} eV. The bottom four Si layers were held frozen; all other atoms were fully relaxed with the residual atomic forces at less than 0.02 eV/Å. This relaxation allows the system to evolve and find equilibrium.

As shown in Figs. 9 and 10, the buckled dimer structure remained largely intact with a slightly reduced tilt angle. We tried to place NaCl molecules parallel to dimer bonds. The relaxed structure was similar to that found in Ref. 26. However, the energy obtained was higher than those shown in Figs. 9 and 10. For (2×2) *A*, NaCl had a local coverage of 0.5 ML and formed nominally flat zigzag chains along the dimer rows. With an increased local NaCl coverage of 0.75 ML, Cl ions, in coherence with the corresponding buckled dimers, tilted up and down in the relaxed (2×4) and (2×2)-*B* structure [Figs. 10(b) and 10(c)]. The NaCl adlayer became rather nonplanar, similar to that found in the KCl/Si(100) system. Unfortunately, ionic species have a low state density near the Fermi level, contributing to tunneling currents, and STM images such as those in Figs. 5(a) cannot resolve and are therefore unable to verify the detailed atomic registry for Na and Cl ions. Instead, STM images predominately show SDBs which have a finite (nonzero) density of states near the Fermi level. Judging from the flatness of the subsequent NaCl double layer shown in Figs. 5 and 8, the nonplanar structures in Figs. 10(b) and 10(c) likely flatten out by the flip-flop motion of buckled dimers.[27]

IV. CONCLUSIONS

We studied the adsorption of NaCl on a Si(100)-(2×1) surface at room temperature up to 2.25 MLs with synchrotron x-ray core-level photoelectron spectroscopy and scanning tunneling microscopy. As $\theta < 0.4$ ML, the XPS and STM results together indicated that more than half of the adsorbed NaCl dissociates to form Si-Cl and adsorbed Na. A wetting adlayer is formed after the deposition of 0.65-ML NaCl. This adlayer consists of Si-Cl, adsorbed Na, NaCl networks, and isolated dangling bonds. Many isolated dangling bonds are grouped into small patches, which exhibit the (2×4) or (2×2) ordered structure. Further deposition above 0.65 ML results in the appearance of double-layer NaCl islands which grow in size on top of the first adlayer. Up to $\theta = 1.8$ MLs, the isolated dangling bonds remain at the interface between the NaCl film and the silicon substrate. With the first adlayer acting as a buffer layer, this system demonstrates that a relaxed film of ionic NaCl solid can be grown on the Si(100) surface despite the 3.6% lattice mismatch.

ACKNOWLEDGMENTS

The authors wish to acknowledge the financial support of Taiwan's National Science Council under Grant No. NSC 99-2119-M-007-005-MY3 (D.S.L.). We are grateful to the National Center for High-Performance Computing of Taiwan for providing computational support.

*Author to whom correspondence should be addressed. dslin@phys.nthu.edu.tw

[1] G. D. Wilk, R. M. Wallace, and J. M. Anthony, J. Appl. Phys. **89**, 5243 (2001).
[2] S. Schintke and W.-D. Schneider, J. Phys.: Condens. Matter **16**, R49 (2004).
[3] K. Saiki, Appl. Surf. Sci. **113-114**, 9 (1997).
[4] C. T. Lou, H. D. Li, J. Y. Chung, D. S. Lin, and T. C. Chiang, Phys. Rev. B **80**, 195311 (2009).
[5] K. Glöckler, M. Sokolowski, A. Soukopp, and E. Umbach, Phys. Rev. B **54**, 7705 (1996).
[6] V. Zielasek, T. Hildebrandt, and M. Henzler, Phys. Rev. B **69**, 205313(2004).
[7] C. A. Lucas, G. C. L. Wong, C. S. Dower, F. J. Lamelas, and P. H. Fuoss, Surf. Sci. **286**, 46 (1993).
[8] H. Guo and R. Souda, J. Appl. Phys. **92**, 6621 (2002).
[9] H. Guo, H. Kawanowa, and R. Souda, Appl. Surf. Sci. **158**, 159 (2000).
[10] M. Katayama, K. Ueno, A. Koma, M. Kiguchi, and K. Saiki, Jpn. J. Appl. Phys., Part 1 **43**, L203 (2004).
[11] S. F. Tsay, J. Y. Chung, M. F. Hsieh, S. S. Ferng, C. T. Lou, and D. S. Lin, Surf. Sci. **603**, 419 (2009).

[12]V. L. Stolyarova, D. U. Sichen, and S. Seetharaman, Vacuum **46**, 871 (1995).
[13]F. J. Himpsel, B. S. Meyerson, F. R. Mc Feely, J. F. Morar, A. Taleb-Ibrahimi, and J. A. Yarmoff, in *Proceeding of the Enrico Fermi School on "Photoemission and Absorption Spectroscopy of Solids and Interfaces with Synchrotron Radiation,"* edited by M. Campagna and R. Rosei (North-Holland, Amsterdam, 1988), p. 203.
[14]E. Landemark, C. J. Karlsson, Y. C. Chao, and R. I. G. Uhrberg, Phys. Rev. Lett. **69**, 1588 (1992).
[15]T.-C. Chiang, Crit. Rev. Solid State Mater. Sci. **14**, 269 (1988).
[16]D. S. Lin, J. L. Wu, S. Y. Pan, and T. C. Chiang, Phys. Rev. Lett. **90**, 046102 (2003).
[17]P. E. J. Eriksson and R. I. G. Uhrberg, Phys. Rev. B **81**, 125443 (2010).
[18]H. Koh, J. W. Kim, W. H. Choi, and H. W. Yeom, Phys. Rev. B **67**, 073306 (2003).
[19]G. A. de Wijs, A. De Vita, and A. Selloni, Phys. Rev. B **57**, 10021 (1998).
[20]P. Gravila and P. F. Meier, Phys. Rev. B **59**, 2449 (1999).
[21]Y. C. Chao, L. S. O. Johansson, and R. I. G. Uhrberg, Phys. Rev. B **55**, 7198 (1997).
[22]B. Voigtländer, T. Weber, P. Šmilauer, and D. E. Wolf, Phys. Rev. Lett. **78**, 2164 (1997).
[23]A. Klust, Q. Yu, M. A. Olmstead, T. Ohta, F. S. Ohuchi, M. Bierkandt, C. Deiter, and J. Wollschläger, Appl. Phys. Lett. **88**, 063107 (2006).
[24]G. Kresse and J. Furthmüller, Phys. Rev. B **54**, 11169 (1996).
[25]G. Kresse and J. Hafner, Phys. Rev. B **49**, 14251 (1994).
[26]A. Maximilian *et al.*, Nanotechnology **20**, 445301 (2009).
[27]J. Nakamura and A. Natori, Phys. Rev. B **71**, 113303 (2005).